The anomalous ionosphere between solar cycles 23 and 24

Stanley C. Solomon,[1] Liying Qian,[1] and Alan G. Burns[1]

Received 16 July 2013; revised 10 September 2013; accepted 10 September 2013; published 1 October 2013.

[1] The solar minimum period during 2008–2009 was characterized by lower thermospheric density than the previous solar minimum and lower than any previously measured. Recent work used the NCAR Thermosphere-Ionosphere-Electrodynamics General Circulation Model to show that the primary cause of density changes from 1996 to 2008 was a small reduction in solar extreme ultraviolet (EUV) irradiance, causing a decrease in thermospheric temperature and hence a contracted thermosphere. There are similar effects in the ionosphere, with most measurements showing an F region ionosphere that is unusually low in density, and in peak altitude. This paper addresses the question of whether model simulations previously conducted, and their solar, geomagnetic, and anthropogenic inputs, produce ionospheric changes commensurate with observations. We conducted a 15 year model run and obtained good agreement with observations of the global mean thermospheric density at 400 km throughout the solar cycle, with a reduction of ~30% from the 1996 solar minimum to 2008–2009. We then compared ionosonde measurements of the midday peak density of the ionospheric F region (N_mF_2) to the model simulations at various locations. Reasonable agreement was obtained between measurements and the model, supporting the validity of the neutral density comparisons. The global average N_mF_2 was estimated to have declined between the two solar minima by ~15%. In these simulations, a 10% reduction of solar EUV plays the largest role in causing the ionospheric change, with a minor contribution from lower geomagnetic activity and a very small additional effect from anthropogenic increase in CO_2.

Citation: Solomon, S. C., L. Qian, and A. G. Burns (2013), The anomalous ionosphere between solar cycles 23 and 24, *J. Geophys. Res. Space Physics*, *118*, 6524–6535, doi:10.1002/jgra.50561.

1. Introduction

[2] The solar minimum period between solar cycles #23 and #24, during the years 2007–2009, was the longest and quietest such period since the advent of space-based measurements, and probably the longest and quietest in a century. Measurements of the solar magnetic field and the interplanetary medium indicated that conditions might be significantly different from previous solar minima [e.g., *Gibson et al*., 2009; *Russell et al*., 2010; *Lockwood*, 2010; *Schrijver et al*., 2011], and changes to the upper atmosphere and ionosphere have been observed and documented, as reviewed below. Additionally, the first half of solar cycle (SC) #24 has also been the weakest since SC #14 and possibly the weakest since the Dalton Minimum in the early 1800s.

[3] The first indication that conditions in the near-Earth space environment were commensurately anomalous came from initial measurements from the Coupled Ion Neutral Dynamics Investigation (CINDI) instrument on the C/NOFS satellite during the summer of 2008 [*Heelis et al*., 2009]. These ionospheric observations showed that ion temperatures and the O^+/H^+ transition height were both lower than expected. Measurements of global mean neutral density derived from a long-term data set of satellite drag observations by *Emmert et al*. [2010] found that thermospheric density during 2008 was also significantly lower than during previous solar minimum periods, and well below the expected secular trend [cf., *Bruinsma and Forbes*, 2010]. These findings motivated further observational and modeling studies to document and explain the changes.

[4] Ionospheric measurement analysis following the Heelis et al. findings began with *Coley et al*. [2010], who further described the equatorial distribution of the CINDI measurements, and compared them with radar data from the Jicamarca Observatory. *Lühr and Xiong* [2010] confirmed these ionospheric results using data from the CHAMP and GRACE satellites, and *Klenzing et al*. [2011] analyzed the global distribution of the contracted ionosphere, and showed that it persisted throughout 2008 and 2009. *Yue et al*. [2013] compared measurements by the Constellation Observing System for Meteorology, Ionosphere, and Climate to the empirical International Reference Ionosphere (IRI) model, finding that the model underestimated the ionosphere during 2008. Turning to ground-based measurements, analyses of ionosonde measurements [e.g., *Chen et al*., 2011, 2012; *Liu et al*., 2011, 2012] found a significant decrease in peak ionospheric densities during the cycle 23/24 minimum, compared

[1]National Center for Atmospheric Research, High Altitude Observatory, Boulder, Colorado, USA.

Corresponding author: S. C. Solomon, National Center for Atmospheric Research, High Altitude Observatory, 1850 Table Mesa Dr., Boulder, CO 80307, USA. (stans@ucar.edu)

2169-9380/13/10.1002/jgra.50561

to previous solar minimum periods. *Araujo-Pradere et al*. [2011] also found such decreases, particularly during daytime, but with significant variability from one station to another, and identified commensurate decreases in total electron content (TEC) measured by dual-frequency GPS receivers. *Bilitza et al*. [2012] compared ionosonde measurements to IRI, pointing out that the model underestimates occurred when the solar $F_{10.7}$ proxy index was employed, but not when the IG12 index is used [cf., *Klenzing et al*., 2011]. This index is based on selected ionosonde measurements of the maximum density of the F_2 peak (N_mF_2) [*Liu et al*., 1983]. However, *Lean et al*. [2011a, 2011b] analyzed measurements of global average TEC obtained from the ground-based dual-frequency GPS network and found that there was no significant change between the 1996 and 2008 levels. They argued that this indicates similar solar EUV levels during the two solar minima, which would imply some other cause for the differences in thermospheric neutral density.

[5] Since the neutral density changes appear to be incontrovertible, the ionosphere is expected to be lower in peak altitude, as well as in peak density. Ionosonde measurements of the peak height of the F_2 region (h_mF_2) are less accurate, and more difficult to calibrate between stations and between epochs, than N_mF_2. *Bremer et al*. [2012], *Mielich and Bremer* [2013], and *Araujo-Pradere* [2013], were able to extract long-term trends from comprehensive h_mF_2 records, finding the 2007–2009 period anomalously lower than the long-term trend. Observations using incoherent scatter radar can accurately obtain peak altitude, and there is some evidence of solar minimum differences based on measurements at the Jicamarca observatory [*Liu et al*., 2012]. Also, the space-based measurements referenced above can be interpreted as the result of a cooler and contracted (as opposed to less dense) ionosphere.

[6] Our previous work on the 2008–2009 solar minimum has attempted to explain the anomalously low thermospheric density observed by *Emmert et al*. [2010] using global dynamical modeling of the thermosphere-ionosphere system [*Solomon et al*., 2010, 2011]. The central challenge of this effort is in deciding how to quantify the solar EUV irradiance input to the model. There is no consensus on how different EUV levels were during the SC #23/#24 minimum from the previous minimum, or from earlier minima, or even if they were different at all. Various well-known solar activity proxy indices and measurements give diverse results. However, the annual average of every available index and measurement is lower during 2008 and again during 2009 than it was during 1996. This is discussed in more detail in section 2.1, below. In *Solomon et al*. [2010], an estimate of a 13% reduction in total EUV energy flux from 1996 to 2008, derived from measurements by the Solar EUV Monitor (SEM) on the Solar and Heliospheric Observatory (SOHO), was used [cf., *Woods*, 2010], resulting in reasonable agreement with the change observed in global mean thermospheric density (~30% at 400 km). In *Solomon et al*. [2010], an EUV change of 10%, based on the Mg II core-to-wing ratio, was employed; by also including the effects of reduced geomagnetic activity, good agreement with the observations was again obtained.

[7] The role of geomagnetic activity in causing the reduced thermospheric density was additionally evaluated by *Weimer et al*. [2011] and *Deng et al*. [2012], using the *Weimer* [2005a, 2005b] empirical model of magnetospheric potential and currents in the ionosphere. Deng et al. estimated that ~25% of the reduction in density from 1996 to 2008 was due to reduction in geomagnetic forcing. The year 2009 was even more quiet geomagnetically than 2008. (The annual average *Ap* was 4 in 2009, as compared to 7 in 2008 and 9 in 1996.) Solar EUV levels were apparently unchanged between 2008 and 2009, and the density in 2009 was lower than 2008 by only a few percent. This indicates that low geomagnetic activity was a secondary contribution to the anomalously low thermospheric density.

[8] Superimposed on the interminimum changes is a slow, long-term decline in thermospheric temperature and density caused by anthropogenic increase in atmospheric CO_2 [e.g., *Roble and Dickinson*, 1989; *Keating et al*., 2000; *Emmert et al*., 2004, 2008; *Marcos et al*., 2005; *Qian et al*., 2006, 2011; *Laštovička et al*., 2006, 2008, 2012]. The effect is greatest during solar minimum, in the range of 3% per decade (modeled) to 5% per decade (observed). This change, although small, was included in the work by *Solomon et al*. [2010, 2011] and is included in the simulations performed for this study. Recently, *Emmert et al*. [2012] have shown evidence that CO_2 is increasing in the lower thermosphere at a higher rate than that in the troposphere, perhaps due to change in turbopause mixing rates. If so, this could help explain why the observed rate of thermospheric change is slightly higher than models predict. However, for the problem of interminimum thermosphere/ionosphere differences, anthropogenic global change is a tertiary contribution.

[9] The purpose of this study is to investigate whether the model simulations that produced good agreement with thermospheric observations also correctly describe ionospheric changes. We have, in past work, evaluated the hypothesis that the primary cause (but not the only cause) of anomalously low thermospheric density during the 2008–2009 solar minimum was the reduced level of solar EUV radiation. If true, this has implications for solar physics, the variability of the solar cycle, and perhaps even the variability of solar output, as discussed at the end of this paper. Therefore, our hypothesis demands testing through comparison to diverse measurements. Here we evaluate the correspondence of our model simulations, using reduced solar EUV, to observations of the F region ionosphere.

2. Data Sources

2.1. Solar Measurements and Indices

[10] Full-disk measurements of the solar EUV irradiance could be used to quantify changes between solar minima. Space-based observations include the Solar EUV Monitor (SEM) [*Judge et al*., 1998] on the Solar and Heliospheric Observatory (SOHO), the Solar EUV Experiment (SEE) on the Thermosphere-Ionosphere-Mesosphere Energetics and Dynamics (TIMED) satellite, [*Woods et al*., 2005] the EUV Variability Experiment (EVE) on the Solar Dynamics Observatory [*Woods et al*., 2011], and several suborbital rocket flights used to calibrate these instruments. Soft X-ray measurements were made by the Student Nitric Oxide Explorer (SNOE) [*Bailey et al*., 2000; *Solomon et al*., 2001] by the Solar Radiation and Climate Experiment (SORCE) [*Woods and Rottman*, 2005]. However, only the SEM has made measurements throughout SC #23, including the 1996 and 2008–2009 solar minima. SEM provides the integrated solar EUV flux in the

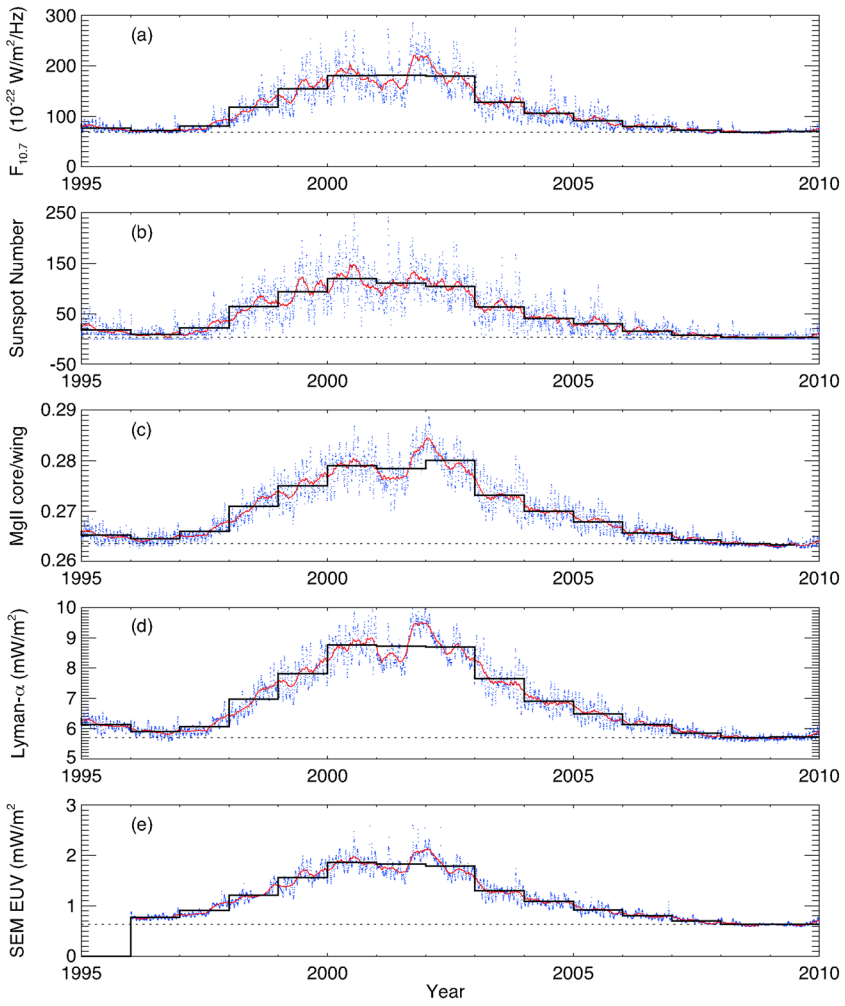

Figure 1. Time series of solar indices and measurements. (a) The 10.7 cm solar radio flux ($F_{10.7}$). (b) Sunspot number (R_z). (c) MgII core-to-wing ratio. (d) H Lyman-α composite index. (e) Solar EUV energy flux in the 26–34 nm band measured by the SEM detector on the SOHO spacecraft. Daily mean values (blue dots). The 81 day centered running means (red lines). Annual means (black solid lines). The 2008 annual means (black dotted lines).

26–34 nm range, which contains the 30.4 nm He II line and several coronal lines. *Didkovsky et al*. [2010] found a reduction from 1996 to 2008 in solar EUV measured by SEM of approximately 15%, with an estimated uncertainty of 6%. Although SEM has been calibrated by eight rocket flights over SC #23, the magnitude of this reduction has been controversial, since it is a somewhat larger change than changes in various proxy indices, as discussed by *Solomon et al*. [2011].

[11] In Figure 1, selected solar indices and measurements are shown for the period 1996–2010. The individual dots are daily values; the blue lines are the 81 day centered running means; the thick black lines are annual averages; the dotted black lines are the 2008 values extended so as to provide a baseline for comparison. The 10.7 cm solar radio flux index $F_{10.7}$ is a popular solar proxy index that correlates well with general solar activity and with EUV and X-ray emissions. It has been used extensively in solar and upper atmosphere empirical models, and is available nearly continuously since 1947 from measurements in Ottawa and Pendicton, Canada [*Covington and Medd*, 1954]. The Zurich Sunspot Number (R_z) is a traditional indicator of the solar activity cycle and also correlates well with solar irradiance on intermediate time scales (1 to 10 solar rotations). The core-to-wing ratio of the magnesium ion *h* and *k* lines at 279.56 and 280.27 nm (MgII c/w) is also a good indicator of solar chromospheric activity, and is a useful proxy for solar irradiance in the UV and EUV wavelengths [*Viereck et al*., 2004, 2010]. It is calculated by taking the ratio between the highly variable chromospheric lines and the weakly varying photospheric wings. Measurements from the NOAA Solar Backscatter Ultraviolet (SBUV) instruments, the Upper Atmosphere Research Satellite (UARS), the Global Ozone Monitoring Experiment (GOME), the Scanning Imaging Absorption Spectrometer (SCIAMACHY), and the Solar Radiation and Climate Experiment (SORCE), were intercalibrated and combined into a daily index by *Viereck et al*. [2004, 2010]. The hydrogen Lyman-α emission at 121.6 nm is the strongest single line in the UV, and has been measured for decades by rockets, the Atmosphere Explorer (AE) series of satellites, the Solar Mesosphere Explorer (SME), UARS, TIMED, and SORCE. A composite index has been compiled by *Woods et al*. [2000] and continued

Table 1. Annual Averages of Various Solar Measurements

Index	1996	2001	2008	R
$F_{10.7}$	72	181	69	−0.028
R_z	8.6	111	2.9	−0.056
MgII c/w	0.2645	0.2785	0.2635	−0.071
Ly-α	5.9	8.7	5.7	−0.071
SEM	0.77	1.83	0.64	−0.123

subsequently, based on careful intercalibration of these measurements and with gaps filled using correlation relationships with $F_{10.7}$ and MgII c/w. The $F_{10.7}$ data shown in Figure 1 were obtained from the NOAA Space Weather Prediction Center Web site; the daily (R_z) values were taken from Solar Influences Data Analysis Center at the Royal Observatory of Belgium; the "NOAA Provisional" MgII c/w file was provided by R. A. Viereck (personal communication, 2011); the Lyman-α composite was downloaded from the LASP Interactive Solar Irradiance Data Center at the University of Colorado; the SOHO SEM 26–34 nm flux was copied from the University of Southern California Space Sciences Center data service.

[12] All of these indices and measurements are lower during 2008–2009 than in 1996, but by varying amounts. (Figure 1 is arranged in increasing order of interminimum variability.) At solar minimum, $F_{10.7}$ is typically fairly constant, while solar EUV irradiance continues to exhibit small variations [e.g., *Barth et al*., 1990; *Woods et al*., 2000]. Similarly, R_z usually becomes zero for some periods of time; during 2008–2009, these periods were exceptionally long. Unlike these indices, MgII c/w and Ly-α do show a significant decline from 1996 to 2008. Also, MgII c/w and Ly-α do not stop varying below a constant plateau at solar minimum, but continue to exhibit some variation. During 2007–2009, much of that variation ceased, but the fairly constant values during 2008 were similar to the lower envelope of the minimum values during 1996. This indicates that the low EUV irradiance levels in time-averaged quantities may have been the result of the unusually persistent quiet conditions, rather than some unprecedented physical regime. It is not surprising that R_z cannot fully capture this, since it is understood that solar activity in various forms continues to vary even when there are no solar magnetic field regions strong enough to create a visible sunspot. Similarly, $F_{10.7}$ may be unable to accurately reflect these low-level variations, since at a value near 66×10^{-22} $\mathrm{Wm^{-2}Hz^{-1}}$ the quiet Sun component produced by Bremsstrahlung emission over the entire Sun dominates the observed emission, as any remaining active regions are no longer strong enough to produce additional radio emissions [*Tapping and DeTracy*, 1990]. Thus, in addition to being unable to represent small variations in solar EUV during solar minimum, $F_{10.7}$ may not be able to quantify interminimum differences when the Sun becomes extremely quiet for an extended period.

[13] In order to compare these indices in a consistent way, we calculate the difference between the annual average value of each index in 2008 and 1996, divided by the expected solar cycle range of the index, as estimated by the difference between the annual average in the solar maximum year of 2001 and in 1996, i.e., $R = [i_{aa}(2008) - i_{aa}(1996)] / [i_{aa}(2001) - i_{aa}(1996)]$. The results of this calculation are given in Table 1.

[14] As previously discussed, the $F_{10.7}$ index shows the least (but still significant) change, and hence cannot be usefully employed in thermosphere-ionosphere models during the 2008–2009 solar minimum. R_z is somewhat better, but has been generally abandoned in favor of indices that correlate better with actual solar EUV levels on a day-to-day basis. Coincidentally, the MgII c/w and Ly-α variations are similar. Caution is indicated, because in both cases these are composites derived from different measurements on different satellites. In the case of Ly-α, the measurements during 1996 are from the SOLSTICE instrument on UARS, and in 2008–2009 from the SOLSTICE instrument on SORCE, and the amount of variation is similar to the measurement uncertainty. However, the use of stellar calibration by the SOLSTICE instruments lends some confidence to the continuity of the measurement. The fact that the Ly-α composite correlates very well with the MgII c/w index supports the choice of MgII c/w as an input to thermosphere-ionosphere models in previous simulations. The interminimum variation measured by SOHO/SEM is an outlier in this group; given the stated uncertainties in time-dependent calibration, this measurement is not completely inconsistent with the MgII c/w and Ly-α composites, but clearly should be used with caution, since there may be issues with secular drift. Therefore, the model simulations described in section 3 employ the MgII c/w as a solar EUV proxy input, using the method described by *Solomon et al*. [2011].

2.2. Ionospheric Measurements

[15] Diverse observational data are available for ionospheric analysis, but relatively few methods provide long-term continuity suitable for secular studies. Previous analyses of different data sources relevant to the comparative solar minimum problem are reviewed in section 1 above. Prominent among these are ionosondes, incoherent scatter radars (ISR), and total electron content (TEC) from dual-frequency GPS. ISR measurements are relatively sparse in distribution and temporal coverage, but provide the best measurements of ionospheric heights. TEC observations have yielded varying results [cf., *Araujo-Pradere et al*., 2011, 2013; *Lean et al*., 2011a, 2011b]. Since ionosondes are numerous, widely distributed, and have a long history of stable operation, we chose to use them for this study. We have utilized a group of ionosondes with minimal overlap to the investigations reviewed in section 1, with data obtained from the World Data Center in Boulder.

[16] The most straightforward and best calibrated quantity derived from ionosonde measurements is the peak density of the F_2 region ionosphere (N_mF_2), which is also generally the peak of the ionospheric density altitude profile. It is derived from the critical frequency f_0F_2 using the well-known relationship $N_mF_2 = 12{,}400(f_0F_2)^2$ (with density in $\mathrm{cm^{-3}}$ and frequency in MHz). Since frequency is an easily calibrated quantity, and since f_0F_2 is relatively simple to identify in ionosonde data by manual or automatic procedures, this is probably the best long-term data source for this type of investigation. The peak E region density N_mE, similarly derived from f_0E, would be an even more direct indication of solar EUV irradiance [e.g., *Buonsanto et al*., 1995], but it is more difficult to extract from ionosonde data than f_0F_2, and is therefore sparse in the data bases.

[17] We have further focused this study on midday measurements of N_mF_2. The rationale for this choice is that the middle of the day is when the ionosphere responds most directly to solar ionization. The F region ionosphere persists at night,

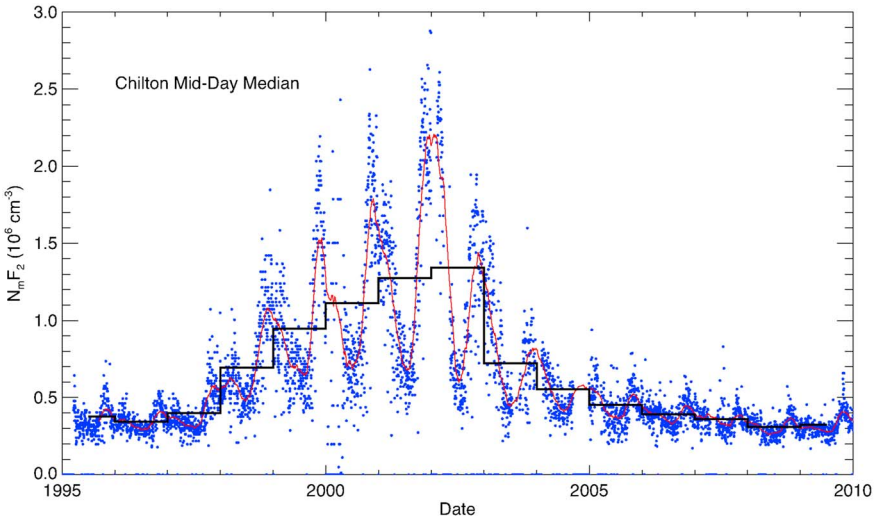

Figure 2. Maximum F region ionospheric density (N_mF_2) measured by the ionosonde at Chilton, United Kingdom. Daily median between 9:00 and 15:00 local time (blue dots). The 81 day centered running mean of the midday medians (red line). Annual averages of the midday medians (thick black line).

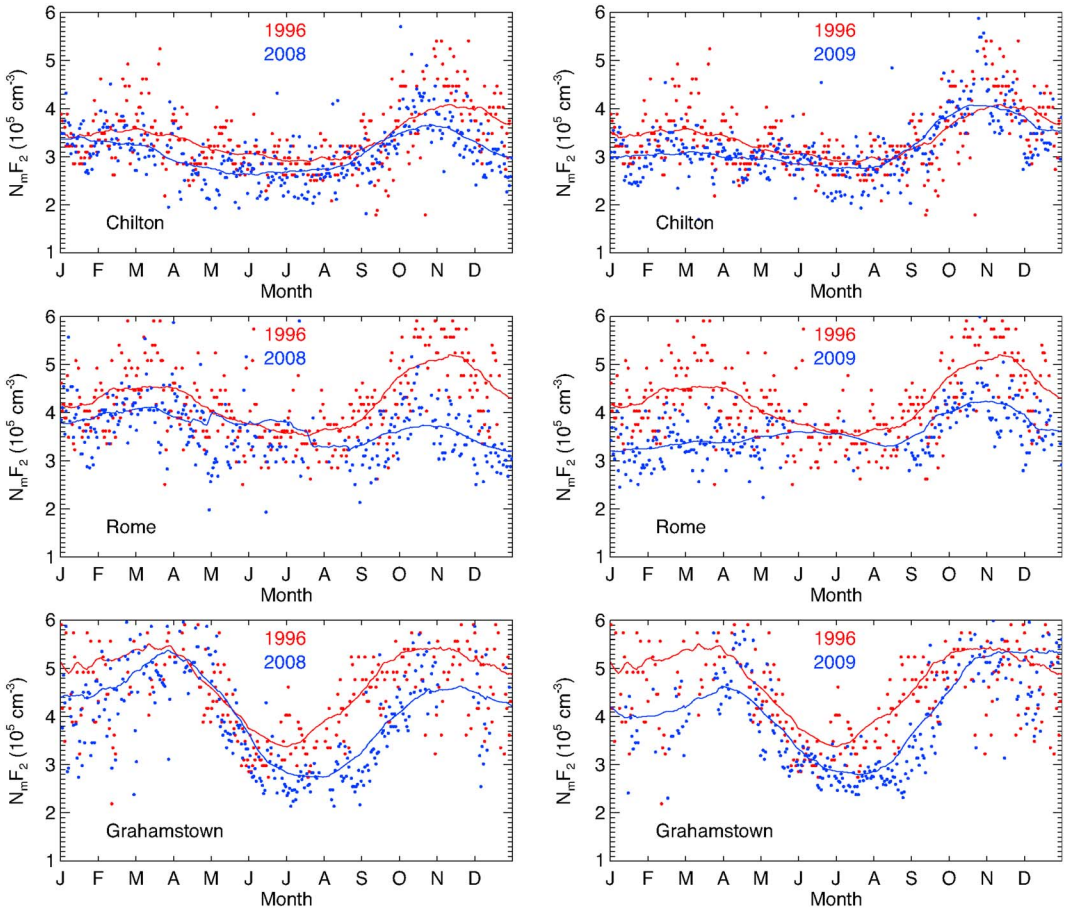

Figure 3. Solar minimum N_mF_2 midday medians at three ionosonde stations, comparing 1996 (red) to 2008 and 2009 (blue) values. Daily median value between 9:00 and 15:00 local time (dots). The 81 day centered running mean of the midday medians (lines). (left column) 1996 compared to 2008. (right column) 1996 compared to 2009. (top row) Chilton, United Kingdom. (middle row) Rome, Italy. (bottom row) Grahamstown, South Africa.

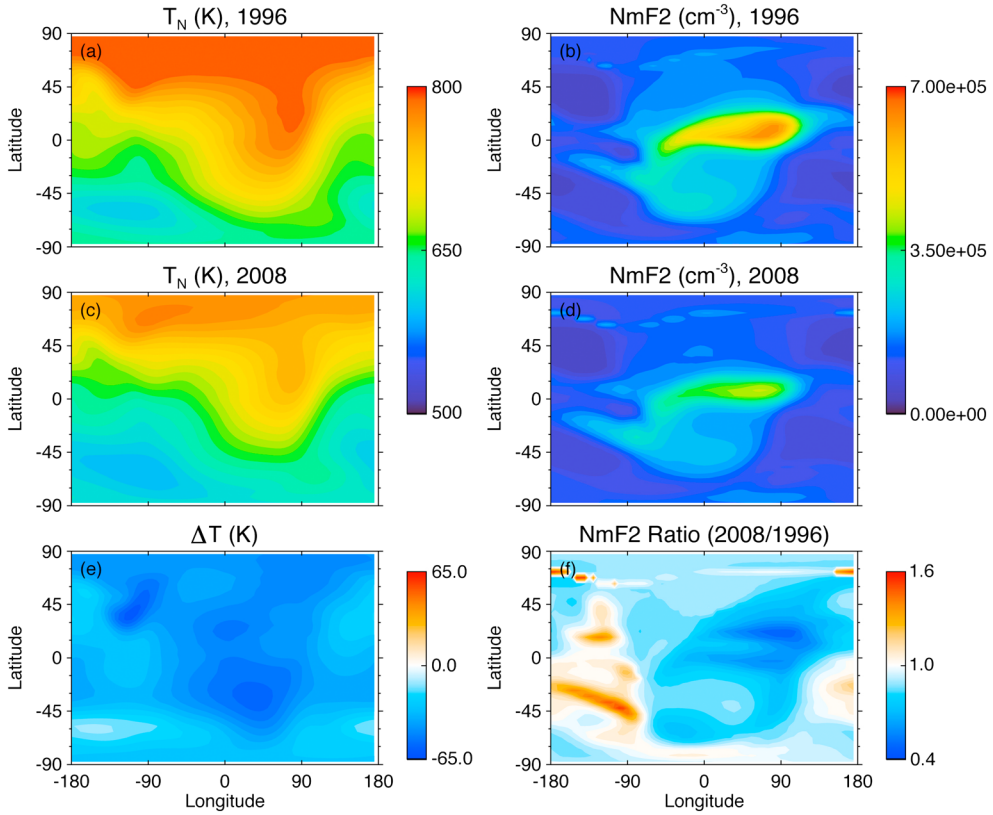

Figure 4. Thermospheric temperature and density modeled by the NCAR TIE-GCM for 1996 and 2008, on day-of-year 180, using the scaled MgII c/w proxy index $M_{10.7}$ as input. (top left) Model exospheric temperature for 1996. (top right) Model peak electron density of the F_2 region N_mF_2 for 1996. (middle left) Model exospheric temperature for 2008. (middle right) Model N_mF_2 for 2008. (bottom left) Exospheric temperature difference, 2008–1996. (bottom right) N_mF_2 ratio at 400 km, 2008/1996.

but declines rapidly, and the lower ionosphere is quite short-lived, so nighttime densities respond strongly to atmospheric and geomagnetic variations and less so to solar forcing. *Araujo-Pradere et al.* [2011, 2013] found interminimum differences in the daytime ionosphere but no significant change at night, which is not surprising in light of the model simulations shown in section 3 below. Therefore, we have chosen to concentrate on daytime measurements. Our procedure was to calculate the median value of the period between 9:00 and 15:00 local solar time, generally similar to the noon value. This eliminates anomalous spikes or dropouts in the data. Days with obviously erroneous (or missing) data were discarded. An example time series of data spanning SC #23, from the station at Chilton, United Kingdom, is shown in Figure 2. The 81 day running centered mean of the midday medians, and the annual (calendar year) mean are also plotted.

[18] In Figure 3, we show examples of data from Chilton and two other stations (Rome, Italy, and Grahamstown, South Africa) during 1996, 2008, and 2009. Daily midday medians and their 81 day running centered mean are plotted, representative of the larger group of measurements summarized below. The left column of Figure 3 compares 1996 to 2008, and the right column compares 1996 to 2009. The seasonal dependence is prominent in these plots (as it is in Figure 2), but 2008 and 2009 are systematically lower. The difference is not large, but it is particularly noticeable from mid-2008 through mid-2009, which was the most quiet period of the SC #23/#24 minimum. We performed this analysis using nine ionosonde stations. These stations were selected because they had minimal overlap with similar analyses in previous work [e.g., *Chen et al.*, 2011, 2012; *Liu et al.*, 2011, 2012; *Araujo-Pradere et al.*, 2011, 2013], and because their World Data Center records contain adequate coverage, at least during the two solar minima. The results and their comparison to model calculations are described in section 4, below.

3. Model Simulations

3.1. Model Description

[19] Model simulations were performed using the NCAR Thermosphere-Ionosphere-Electrodynamics General Circulation model (TIE-GCM) v. 1.94 [*Roble et al.*, 1988; *Richmond et al.*, 1992]. The TIE-GCM is a first-principles upper atmospheric general circulation model that solves the Eulerian continuity, momentum, and energy equations for the coupled thermosphere-ionosphere system. The vertical coordinate is pressure levels in half-scale height intervals, extending in altitude from approximately 97 km to 600 km, depending on solar activity. Tidal forcing at the lower boundary was specified by the Global Scale Wave Model [*Hagan et al.*, 2001], and semiannual and annual density periodicities were obtained by applying seasonal variation of the eddy diffusivity coefficient at the lower boundary [*Qian et al.*, 2009, 2013]. The CO_2 mixing ratio imposed at the lower boundary was 364 ppmv for 1996, increasing linearly by

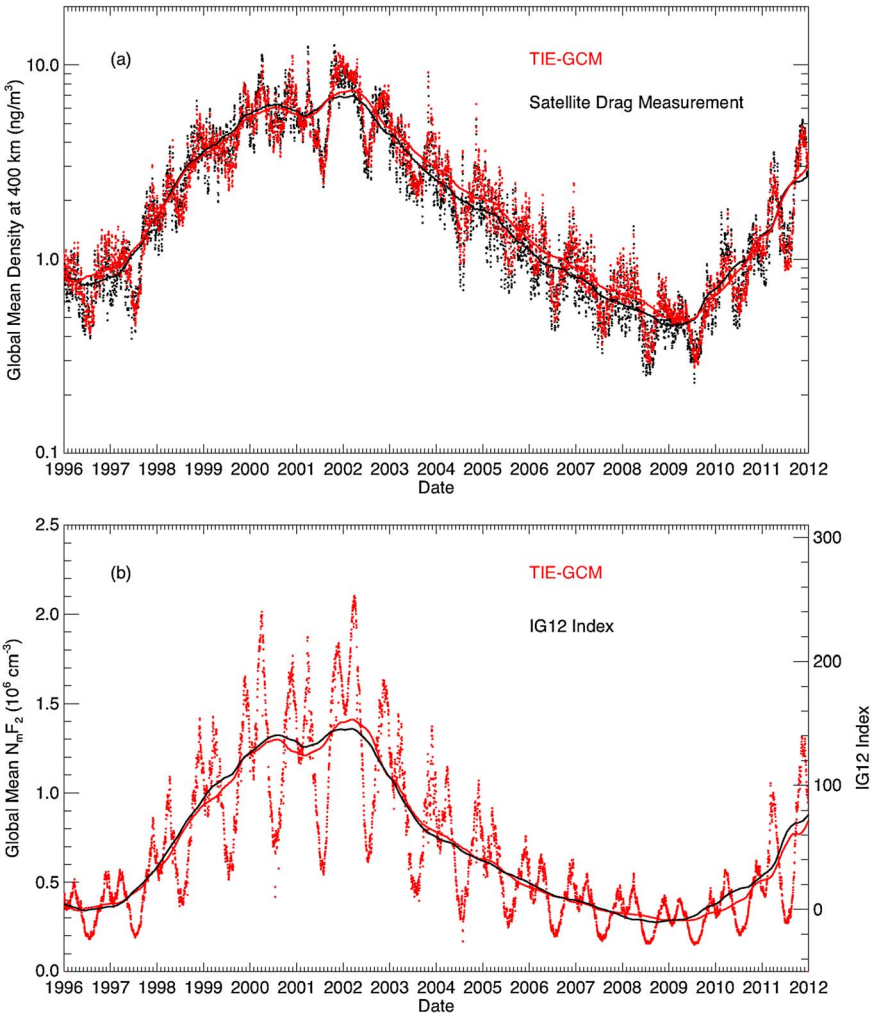

Figure 5. (a) Comparison of modeled and measured global mean neutral density at 400 km. Simulations by the NCAR TIE-GCM (red). Measurement through analysis of atmospheric drag on orbiting objects (black) [*Emmert*, 2009]. Daily values (dots). 365 day centered running mean (lines). (b) Comparison of modeled global mean N_mF_2 to the IG12 index. Simulations by the NCAR TIE-GCM (red). Daily values (red dots). 365 day centered running mean (red line). IG12 index (black line).

1.5 ppmv per year, based on measurements from the Mauna Loa Observatory [*Keeling and Whorf*, 2005].

[20] Magnetospheric inputs to the polar regions are specified by an applied electric potential pattern and an auroral precipitation oval. The *Heelis et al.* [1982] empirical specification of magnetospheric potential in the ionosphere, which is parameterized by the geomagnetic K_p index, is the standard TIE-GCM input. Auroral precipitation is applied as described by *Roble and Ridley* [1987] based on the estimated hemispheric power of precipitating electrons. The empirical estimate of this power as it depends on K_p has been increased from the original formulation by a factor of ~2, based on results from the Global Ultraviolet Imager (GUVI) on the TIMED satellite [*Zhang and Paxton*, 2008]. TIE-GCM v. 1.94 also has the option of applying the *Weimer* [2005a, 2005b] convection pattern. In this case, hemispheric power is calculated as a function of the north-south component of the interplanetary magnetic field B_z and the solar wind speed [*Emery et al.*, 2009], adjusted to match GUVI calculations by multiplying the Emery et al. formula by a factor of 2. The TIE-GCM calculates the low-latitude ionospheric electrodynamo driven by conductances and neutral dynamics, using the method of *Richmond et al.* [1992]. The calculated electric potential is merged with the externally imposed potential within each polar cap, using crossover boundaries that vary dynamically with the size of the magnetospheric potential pattern. For the simulations presented here, the Heelis et al. potential, parameterized by K_p, is employed. See *Solomon et al.* [2012, section 2.3], for further detail concerning the high-latitude inputs, and *Solomon et al.* [2011, section 4], for a discussion of model uncertainties.

[21] An ad hoc method was developed for using the MgII c/w ratio in standard solar EUV proxy models. Daily average values of $F_{10.7}$ were compared to MgII c/w during 1978–2007, and an unweighted linear least squares fit of $F_{10.7}$ to MgII c/w performed, resulting in the relationship:

$$M_{10.7} = 7984(\text{MgII c/w}) - 2041 \quad (1)$$

where $M_{10.7}$ is the MgII c/w scaled to $F_{10.7}$, in units of 10^{-22} $\text{Wm}^{-2}\text{Hz}^{-1}$ (see *Solomon et al.* [2011] for further details.)

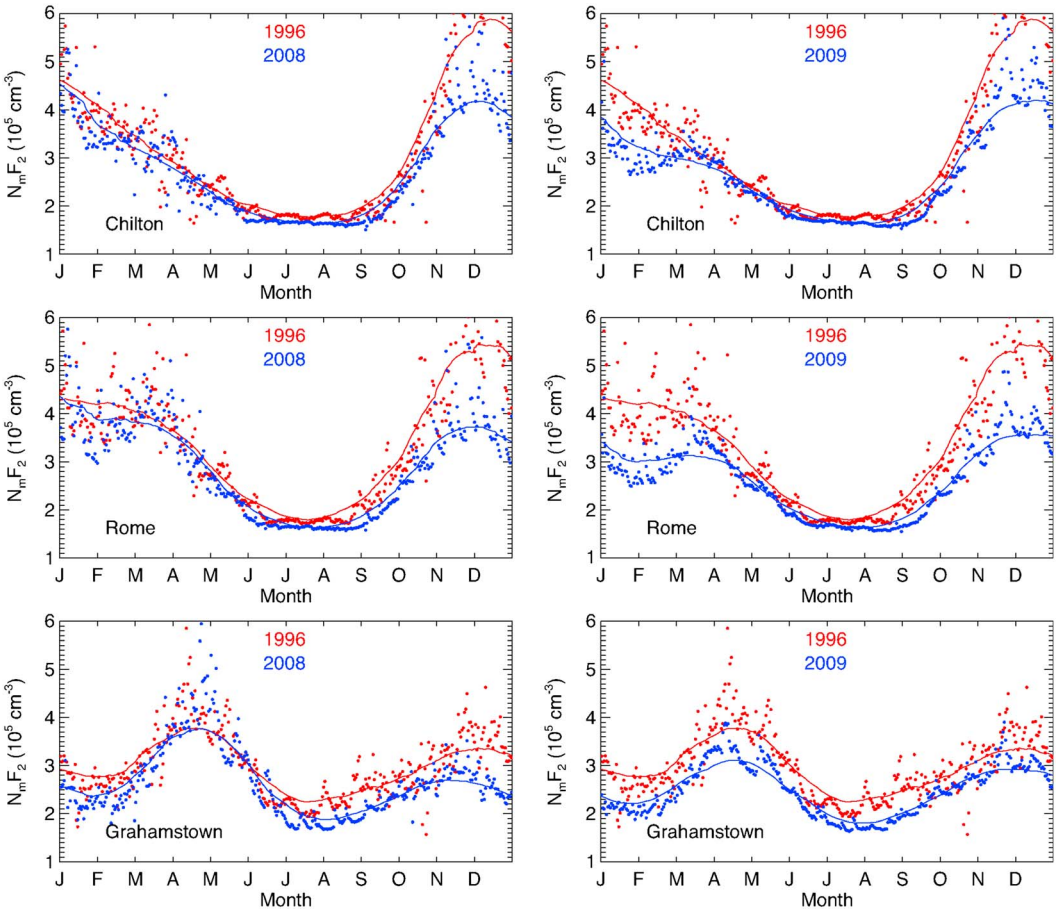

Figure 6. Solar minimum N_mF_2 at 12:00 local time, as simulated by the NCAR TIE-GCM at the locations of the three ionosonde stations shown in Figure 3, comparing 1996 (red) to 2008 and 2009 (blue) values. Daily values (dots). The 81 day centered running mean of the daily values (lines). (left column) 1996 compared to 2008. (right column) 1996 compared to 2009. (top row) Chilton, United Kingdom. (middle row) Rome, Italy. (bottom row) Grahamstown, South Africa.

The standard solar EUV irradiance input to the NCAR TIE-GCM is provided by the EUV for Aeronomic Calculations (EUVAC) proxy model [*Richards et al*., 1994]. The model is extended below 5 nm as described in *Solomon and Qian* [2005]. Individual bands and lines of solar EUV photon flux are calculated by EUVAC as linear functions of the input variable P, which is defined as the average of the daily $F_{10.7}$ and its running 81 day centered mean. For these simulations, we calculated P using $M_{10.7}$ and its 81 day mean, and used it as input to EUVAC. Similarly, far ultraviolet (FUV) irradiances are provided by the *Woods and Rottman* [2002] model, which also employs daily $F_{10.7}$ and its 81 day mean; these values were likewise calculated by substituting $M_{10.7}$. The annual mean EUV energy flux derived from $M_{10.7}$ is 10% lower in 2008 than in 1996, as compared to only 4% lower using $F_{10.7}$. The FUV flux has much less variability, and hence is only slightly different for the two input proxies.

3.2. Model Results

[22] The TIE-GCM was run for 15 years, from 1996 through 2011, all of SC #23 and the rising phase of SC #24. Examples of these simulations are shown in Figure 4. Neutral temperature at 400 km, essentially the exospheric temperature and N_mF_2 are plotted for a day near northern summer solstice in 1996 and 2008. The temperature difference and the N_mF_2 ratio are also shown. The systematic reduction in both quantities is particularly strong during the day, as expected; but in some locations N_mF_2 actually increases during the night. The temperature change is fairly uniform, but N_mF_2 exhibits considerable structure. This exemplifies the complexity of ionospheric analysis—although thermospheric change was systematic, ionospheric change depends on location, time of day, season, and geophysical conditions. Under sunlit conditions, the decrease in ionization rate dominates the other influences, but at night, changes in composition, temperature, and neutral winds have diverse impacts. The global mean annual average reduction in N_mF_2, comparing 1996 to 2008, was 15%, i.e., a ratio of 0.85. The global mean annual average h_mF_2 decreased by 9 km.

[23] In Figure 5a, global mean neutral density simulations are compared to satellite drag measurements at 400 km [*Emmert*, 2009]. The solar cycle, seasonal, and interminimum variations are consistent, and even the response to major geomagnetic events is approximately correct (e.g., note the peaks in October 2003 and November 2004). Figure 5b similarly compares the global mean N_mF_2 to the IG12 index. This index

Table 2. Comparison of Median Midday N_mF_2 Ratios at Ionosonde Stations

Station	Geo. Lat.	Geo. Long.	Mag. Lat.	Measured 2008/1996	Modeled 2008/1996	Measured 2009/1996	Modeled 2009/1996
Juliusruh	55	13	51	0.88	0.91	0.92	0.91
Chilton	52	−1	48	0.88	0.91	0.93	0.91
Eglin	30	−87	41	0.93	0.82	-	0.72
Point Arguello	35	−121	40	1.01	0.87	0.89	0.81
Rome	42	13	36	0.84	0.89	0.80	0.82
Del'Ebre	41	0	35	1.10	0.90	1.06	0.83
Learmonth	−22	114	−33	0.85	0.84	0.86	0.72
Grahamstown	−33	27	−42	0.86	0.88	0.87	0.83
Hobart	−43	147	−54	0.91	0.88	0.95	0.85

is derived from ionosonde measurements of N_mF_2, similar to the analysis presented here, and scaled to the range of R_z values, specifically for use in models such as IRI [*Liu et al*., 1983]. As pointed out by *Klenzing et al*. [2011], this index actually goes negative during the SC #23/#24 solar minimum, which of course is impossible for R_z. The index was obtained from the IRI web site at the NASA Goddard Space Flight Center, as provided by the World Data Center at the Rutherford Appleton Laboratory, Chilton, United Kingdom. In its standard formulation, it is subjected to a 12 month centered running mean, to eliminate the prominent seasonal changes. Because the scaling between N_mF_2 and IG12 in Figure 5b is arbitrary, not too much should be made of the good correspondence on a 12 month smoothed basis between model and index, other than the fact that IG12 shows a decline from 1996 to 2008–2009 similar to the solar indices employed, the model simulations, and observations from individual ionosonde stations. The stations contributing to the index have evolved over the years, so its secular stability is questionable, similar to the situation with global mean TEC derived from GPS measurements. Therefore, we compare solar minimum model simulations to individual station measurements in the following section.

4. Comparison of Simulations to Measurements

[24] Figure 6 displays the results of model simulations for 1996, 2008, and 2009 at three of the ionosonde stations used in the analysis (Chilton, United Kingdom, Rome, Italy, and Grahamstown, South Africa). Comparison to Figure 3 reveals that the model still struggles to accurately capture the seasonal climatology of the amplitude and phase of the well-known annual and semiannual variations [*Burns et al*., 2012; *Qian et al*., 2013]. However, since the *Qian et al*. [2009] lower boundary condition is employed, these variations are at least present. The simulations for Chilton have about the right seasonal morphology, and those for Rome are quite reasonable. In both cases, the model underestimates the summer values. At Grahamstown, the model is low overall, although the amplitude and phase of the seasonal variations are about right. The offsets between 1996 and 2008–2009 are clear, and agree with the data in general. The reductions were small during early 2008, and largely nonexistent during the last gasp of SC #23 in April 2008. The differences are largest from mid-2008 to late-2009, and then start to recover as SC #24 picks up. Averaged over time, the model change is very similar to the measured change.

[25] The results for measurements and models at the locations of the nine selected ionosonde stations, at solar minimum, are shown in Table 2. This table summarizes the annual medians of the ratio of daily midday medians during 2008 to the same day in 1996, for the measurements and the model. For the measurements, days when data were missing from either year were excluded from the analysis. The comparison is repeated comparing 2009 to 1996. The table is organized by decreasing magnetic latitude (i.e., from north to south). The measurements show considerably more scatter than the model, as would be expected, but the comparison is quite good in most cases, and the systematic reduction in daytime N_mF_2 is clear. The outliers are the measurements at Del'Ebre, Spain, which are included even though the seasonal pattern during 2008 and 2009 is quite different from 1996, showing a spurious summertime peak not generally observed with other ionosondes. The measurements at Juliusruh, Germany closely track those at Chilton, which is reassuring, considering that they are only about 800 km apart. Data from Eglin, US, were not available during 2009. Hobart, the station highest in magnetic latitude, has fairly small measured changes, somewhat discrepant from the model calculation, but there are not enough samples to determine whether there is a systematic magnetic latitude effect.

[26] A similar analysis by *Chen et al*. [2011] for six ionosonde stations (different ones from those in Table 2) found ratios in the range 0.67 to 0.85, slightly larger reductions than those measured or modeled here. *Liu et al*. [2011] found commensurate reductions through analysis of a larger set of ionosonde stations, resulting in ratios averaging about 0.85, very similar to our simulations. These results were also comparable to those of *Araujo-Pradere et al*. [2011], at least for daytime measurements.

5. Conclusions

[27] The evidence that the thermosphere was lower in density during 2008–2009 than during the previous solar minimum is overwhelming, so the only controversial aspect is the attribution of causation. The evidence that the density of the daytime F_2 ionosphere was also lower in density is merely compelling. Due to the more complex ionospheric morphology, and the lack of a single long-term measurement as reliable as the satellite drag data, it is more difficult to quantify, but almost every ionosonde station evaluated shows a decline. The height of the maximum density in the ionosphere h_mF_2 must also have been lower, regardless of the cause of the low thermospheric densities, because either a reduction in temperature or a reduction in atomic oxygen density will have the same effect of lowering the ionospheric altitude, which largely follows pressure surfaces. A dozen publications, reviewed in section 1 above, document the ionospheric changes between the two solar minima.

[28] In this work, we have shown that the same model input assumptions regarding solar, geomagnetic, and anthropogenic forcing of the upper atmosphere that produce good agreement with global mean thermospheric density change produce good agreement with the magnitude of ionospheric changes, although getting the ionospheric spatial and seasonal morphology correct remains challenging. In our simulations, solar EUV is the largest driver of these changes, and it is the change in solar ionization rate (which drives thermospheric heating and hence temperature and density as well as the daytime ionosphere) that causes most of the difference between the solar minima. This reduction in solar EUV is not large, now estimated at 10% or even less, but the effect on thermospheric density increases with altitude, so that it is quite significant (~30%) near 400 km, while the ionospheric reduction is more modest, probably less than half that amount.

[29] The self-consistency of our model simulations does not rule out other possible causes of interminimum differences. For instance, a change in atomic-to-molecular composition can have a similar effect on the thermosphere and ionosphere, since less atomic oxygen means lower thermospheric density, and also reduces ionospheric density by increasing chemical loss rates in the F region. However, the thermosphere appears to be following the usual relationship with solar EUV proxies such as $F_{10.7}$ during the rising phase of SC #24, so secular decrease in atomic oxygen seems unlikely. Another aspect of causation attribution is the contribution of geomagnetic activity. Auroral precipitation and Joule heating from magnetospheric currents heat the thermosphere, and some part of the interminimum differences may have been due to the more quiet geomagnetic conditions. The contribution has been variously estimated to be causing on the order of a quarter of the interminimum density reduction (see section 1 above). It is unlikely to have been much more significant than that, based partly on comparison of 2008 and 2009. The annual average *Ap* index was 9 in 1996, 7 in 2008, and 4 in 2009, but 2009 was only 5% lower in density than 2008. Large auroral storms cause significant ionospheric perturbations, but the lower-level activity during solar minimum, caused by high-speed streams in the solar wind, and the associated corotating interaction regions, has a much more muted effect on global ionospheric densities than on thermospheric densities [cf., *Solomon et al*., 2012]. Geomagnetic forcing was included in our simulations, so it does make a minor contribution to the ionospheric changes shown here. The contribution from global change due to anthropogenic CO_2 and other greenhouse gases is even smaller, especially in the ionosphere, since N_mF_2 is weakly dependent on these changes [e.g., *Qian et al*., 2008].

[30] The empirical IRI model also demonstrates that solar-driven changes in the ionosphere are more significant during the day, which is why the IG12 index is based on noon measurements of N_mF_2. This is consistent with our analyses, and also with common sense, since the night ionosphere undergoes rapid decay (depending on altitude) and responds to composition, winds, and chemical rates in addition to the residual solar ionization that caused it.

[31] The one piece of evidence contradicting these conclusions is the behavior of the global average total electron content (TEC) obtained from GPS data [*Lean et al*., 2011a, 2011b]. There are several reasons why TEC might not behave in the same manner as N_mF_2. TEC observations using this method include most of the plasmasphere, and it is not clear how the plasmasphere responds to solar EUV and geomagnetic activity, particularly at solar minimum, and particularly at night, when the plasmasphere contribution to TEC can be as large as the ionosphere [cf., *Lee et al*., 2013]. The global mean TEC measurement has been shown to correlate well with solar proxy indices such as $F_{10.7}$ in the past, but the number of stations contributing to the measurement has increased drastically since it began in 1995.

[32] In summary, we find that model simulations which produced good agreement with global mean thermospheric density are also consistent with most ionospheric data. We have extended the model runs to cover 15 years, or about 1.5 solar cycles, and have obtained good agreement with both the solar cycle variation and the interminimum changes in thermospheric density. The variations produced in the ionosphere are commensurate with measurements, which supports the validity of the simulations. Ultimately, the changes in the thermosphere-ionosphere system were mostly caused by the Sun.

6. Discussion

[33] Solar EUV radiation is produced in magnetically active regions on the Sun, so it should not be surprising that a solar minimum that was unusually long and unusually "quiet" with respect to solar magnetic activity should also produce less EUV. The questions are, what does "unusual" mean in this context, and do these findings have any implications for other regions of the solar spectrum? We have confined this study to the comparison of the solar minima between SC #22 and #23, and between SC #23 and #24, but the presumption that previous solar minima were fundamentally similar forms the basis for our claim that the most recent one was anomalous. SC #24 has been weak as well as late, and may already be in its declining phase. This has fueled speculation that the Sun is entering something resembling the Dalton Minimum of the early 1800s, or even a new Maunder Minimum [*Eddy*, 1976]. How the solar spectrum changes on decadal or centurion time scales is a central question for upper atmospheric science, and perhaps for atmospheric science in general. The difficulties and controversies surrounding the endeavor to compare solar and geospace parameters between 1996 and 2008–2009 have been instructive. We now have comprehensive, well-calibrated measurements for 2008–2009. Will we have the vision to prepare for 2020?

[34] **Acknowledgments.** The authors thank John Emmert and colleagues for providing the thermospheric neutral density data, Thomas Woods and colleagues for providing SEE and EVE data, Leonid Didkovsky and colleagues for providing SEM data, and Rodney Viereck for providing the MgII c/w index compilation. This research was supported by NASA grants NNX10AF21G and NNX07AC61G to the National Center for Atmospheric Research. NCAR is supported by the National Science Foundation.

[35] Robert Lysak thanks the reviewers for their assistance in evaluating this paper.

References

Araujo-Pradere, E. A., R. Redmon, M. Fedrizzi, R. Viereck, and T. J. Fuller-Rowell (2011), Some characteristics of the ionospheric behavior during solar cycle 23/24 minimum, *Solar Phys.*, *274*, 439, doi:10.1007/s11207-011-9728-3.

Araujo-Pradere, E. A., D. Buresova, D. J. Fuller-Rowell, and T. J. Fuller-Rowell (2013), Initial results of the evaluation of IRI hmF2 performance for minima 22–23 and 23–24, *Adv. Space Res.*, *51*, 630–638.

Bailey, S. M., T. N. Woods, C. A. Barth, S. C. Solomon, L. R. Canfield, and R. Korde (2000), Measurements of the solar soft X-ray irradiance from the Student Nitric Oxide Explorer: First analysis and underflight calibrations, *J. Geophys. Res.*, *105*, 27,179–27,193.

Barth, C. A., W. K. Tobiska, G. J. Rottman, and O. R. White (1990), Comparison of 10.7 cm radio flux with SME solar Lyman alpha flux, *Geophys. Res. Lett.*, *17*, 571, doi:10.1029/GL017i005p00571.

Bilitza, D., S. A. Brown, M. Y. Wang, J. R. Souza, and P. A. Roddy (2012), Measurements and IRI model predictions during the recent solar minimum, *J. Atmos. Sol. Terr. Phys.*, *86*, 99, doi:10.1016/j.jastp.2012.06.010.

Bremer, J., T. Damboldt, J. Mielich, and P. Suessmann (2012), Comparing long-term trends in the ionospheric F2-region with two different methods, *J. Atmos. Sol. Terr. Phys.*, *77*, 174, doi:10.1016/j.jastp.2011.12.017.

Bruinsma, S. L., and J. M. Forbes (2010), Anomalous behavior of the thermosphere during solar minimum observed by CHAMP and GRACE, *J. Geophys. Res.*, *115*, A11323, doi:10.1029/2010JA015605.

Buonsanto, M. J., P. G. Richards, W. K. Tobiska, S. C. Solomon, Y.-K. Tung , and J. A. Fennelly (1995), Ionospheric electron densities calculated using different EUV flux models and cross sections: Comparison with radar data, *J. Geophys. Res.*, *100*, 14,569–14,580.

Burns, A. G., S. C. Solomon, W. Wang, L. Qian, Y. Zhang, and L. J. Paxton (2012), Daytime climatology of ionospheric N_mF_2 and h_mF_2 from COSMIC data, *J. Geophys. Res.*, *117*, A09315, doi:10.1029/2012JA017529.

Chen, Y., L. L. Liu, and W. Wan (2011), Does the F10.7 index correctly describe solar EUV flux during the deep solar minimum of 2007–2009?, *J. Geophys. Res.*, *116*, A04304, doi:10.1029/2010JA016301.

Chen, Y., L. Liu, and W. Wan (2012), The discrepancy in solar EUV-proxy correlations on solar cycle and solar rotation timescales and its manifestation in the ionosphere, *J. Geophys. Res.*, *117*, A03313, doi:10.1029/2011JA017224.

Coley, W. R., R. A. Heelis, M. R. Hairston, G. D. Earle, M. D. Perdue, R. A. Power, L. L. Harmon, B. J. Holt, and C. R. Lippincott (2010), Ion temperature and density relationships measured by CINDI from the C/NOFS spacecraft during solar minimum, *J. Geophys. Res.*, *115*, A02313, doi:10.1029/2009JA014665.

Covington, A. E., and W. J. Medd (1954), Variations of the daily level of the 10.7-centimetre solar emission, *J. R. Astron. Soc. Can.*, *48*, 136.

Deng, Y., Y. Huang, S. C. Solomon, L. Qian, D. J. Knipp, and D. R. Weimer (2012), Anomalously low geomagnetic energy inputs during 2008 solar minimum, *J. Geophys. Res.*, *117*, A09307, doi:10.1029/2012JA018039.

Didkovsky, L. V., D. L. Judge, and S. R. Wieman (2010), Minima of solar cycles 22/23 and 23/24 as seen in SOHO/CELIAS/SEM absolute solar EUV flux, in *ASP Conference Series, SOHO-23: Understanding a Peculiar Solar Minimum*, S. R. Cranmer, J. T. Hoeksema, and J. Kohl, eds., vol. 428, p. 73, http://arxiv.org/PS_cache/arxiv/pdf/0911/0911.0870v1.pdf.

Eddy, J. A. (1976), The Maunder Minimum, *Science*, *192*, 4245.

Emery, B. A., I. G. Richardson, D. S. Evans, and F. J. Rich (2009), Solar wind structure sources and periodicities of auroral electron power over three solar cycles, *J. Atmos. Sol. Terr. Phys.*, *71*(10–11), 1157–1175, doi:10.1016/j.jastp.2008.08.005.

Emmert, J. T. (2009), A long-term data set of globally averaged thermospheric total mass density, *J. Geophys. Res.*, *114*, A06315, doi:10.1029/2009JA014102.

Emmert, J. T., J. M. Picone, J. L. Lean, and S. H. Knowles (2004), Global change in the thermosphere: Compelling evidence of a secular decrease in density, *J. Geophys. Res.*, *109*, A02301, doi:10.1029/2003JA010176.

Emmert, J. T., J. M. Picone, and R. R. Meier (2008), Thermospheric global average density trends, 1967–2007, derived from orbits of 5000 near-Earth objects, *Geophys. Res. Lett.*, *35*, L05101, doi:10.1029/2007GL032809.

Emmert, J. T., J. L. Lean, and J. M. Picone (2010), Record-low thermospheric density during the 2008 solar minimum, *Geophys. Res. Lett.*, *37*, L12102, doi:10.1029/2010GL043671.

Emmert, J. T., M. H. Stevens, P. F. Bernath, D. P. Drob, and C. D. Boone (2012), Observations of increasing carbon dioxide concentration in Earth's thermosphere, *Nat. Geosci.*, *5*, 868–871, doi:10.1038/NGEO1626.

Gibson, S. E., J. U. Kozyra, G. de Toma, B. A. Emery, T. Onsager, and B. J. Thompson (2009), If the Sun is so quiet, why is the Earth ringing? A comparison of two solar minimum intervals, *J. Geophys. Res.*, *114*, A09105, doi:10.1029/2009JA014342.

Hagan, M. E., R. G. Roble, and J. Hackney (2001), Migrating thermospheric tides, *J. Geophys. Res.*, *106*(A7), 12,739–12,752.

Heelis, R. A., J. K. Lowell, and R. W. Spiro (1982), A model of the high-latitude ionosphere convection pattern, *J. Geophys. Res.*, *87*(A8), 6339–6345.

Heelis, R. A., W. R. Coley, A. G. Burrell, M. R. Hairston, G. D. Earle, M. D. Perdue, R. A. Power, L. L. Harmon, B. J. Holt, and C. R. Lippincott (2009), Behavior of the O^+/H^+ transition height during the extreme solar minimum of 2008, *Geophys. Res. Lett.*, *36*, L00C03, doi:10.1029/2009GL038652.

Judge, D. L., et al. (1998), First solar EUV irradiances obtained from SOHO by the CELIAS/SEM, *Solar Phys.*, *177*, 161.

Keating, G. M., R. H. Tolson, and M. S. Bradford (2000), Evidence of long-term global decline in the Earth's thermospheric densities apparently related to anthropogenic effects, *Geophys. Res. Lett.*, *27*, 1523–1526.

Keeling, C. D., and T. P. Whorf (2005), Atmospheric CO_2 records from sites in the SIO air sampling network, in *Trends: A Compendium of Data on Global Change*, Carbon Dioxide Information Analysis Center, Oak Ridge National Laboratory, U.S. Department of Energy, Oak Ridge, Tenn.

Klenzing, J., F. Simões, S. Ivanov, R. A. Heelis, D. Bilitza, R. Pfaff, and D. Rowland (2011), Topside equatorial ionospheric density and composition during and after extreme solar minimum, *J. Geophys. Res.*, *116*, A12330, doi:10.1029/2011JA017213.

Laštovička, J., R. A. Akmaev, G. Beig, J. Bremer, and J. T. Emmert (2006), Global change in the upper atmosphere, *Science*, *314*, 1253.

Laštovička, J., R. A. Akmaev, G. Beig, J. Bremer, J. T. Emmert, C. Jacobi, M. J. Jarvis, G. Nedoluha, Y. I. Portnyagin, and T. Ulich (2008), Emerging pattern of global change in the upper atmosphere and ionosphere, *Ann. Geophys.*, *26*, 1255.

Laštovička, J., S. C. Solomon, and L. Qian (2012), Trends in the neutral and ionized upper atmosphere, *Space Sci. Rev.*, *168*, doi:10.1007/s11214-011-9799-3.

Lean, J. L., J. T. Emmert, J. M. Picone, and R. R. Meier (2011a), Global and regional trends in ionospheric total electron content, *J. Geophys. Res.*, *116*, A00H04, doi:10.1029/2010JA016378.

Lean, J. L., R. R. Meier, J. M. Picone, and J. T. Emmert (2011b), Ionospheric total electron content: Global and hemispheric climatology, *J. Geophys. Res.*, *116*, A10318, doi:10.1029/2011JA016567.

Lee, H.-B., G. Jee, Y. H. Kim, and J. S. Shim (2013), Characteristics of global plasmaspheric TEC in comparison with the ionosphere simultaneously observed by Jason-1 satellite, *J. Geophys. Res. Space Physics*, *118*, 935–946, doi:10.1002/jgra.50130.

Liu, R. Y., P. A. Smith, and J. W. King (1983), A new solar index which leads to improved foF2 predictions using the CCIR atlas, *Telecommunication Journal*, *50*(8), 408.

Liu, L., Y. Chen, H. Le, V. I. Kurkin, N. M. Polekh, and C.-C. Lee (2011), The ionosphere under extremely prolonged low solar activity, *J. Geophys. Res.*, *116*, A04320, doi:10.1029/2010JA016296.

Liu, L., J. Yang, H. Le, Y. Chen, W. Wan, and C.-C. Lee (2012), Comparative study of the equatorial ionosphere over Jicamarca during recent two solar minima, *J. Geophys. Res.*, *117*, A01315, doi:10.1029/2011JA017215.

Lockwood, M. (2010), Solar change and climate: An update in the light of the current exceptional solar minimum, *Proc. R. Soc. A*, *466*(2114), 303, doi:10.1098/rspa.2009.0519.

Lühr, H., and C. Xiong (2010), IRI-2007 model overestimates electron density during the 23/24 solar minimum, *Geophys. Res. Lett.*, *37*, L23101, doi:10.1029/2010GL045430.

Marcos, F. A., J. O. Wise, M. J. Kendra, N. J. Grossbard, and B. R. Bowman (2005), Detection of a long-term decrease in thermospheric neutral density, *Geophys. Res. Lett.*, *32*, L04103, doi:10.1029/2004GL021269.

Mielich, J., and J. Bremer (2013), Long-term trends in the ionospheric F2 region with different solar activity indices, *Ann. Geophys.*, *31*, 291–303, doi:10.5194/angeo-31-291-2013.

Qian, L., R. G. Roble, S. C. Solomon, and T. J. Kane (2006), Calculated and observed climate change in the thermosphere, and a prediction for solar cycle 24, *Geophys. Res. Lett.*, *33*, L23705, doi:10.1029/2006GL027185.

Qian, L., S. C. Solomon, R. G. Roble, and T. J. Kane (2008), Model simulations of global change in the ionosphere, *Geophys. Res. Lett.*, *35*, L07811, doi:10.1029/2007GL033156.

Qian, L., S. C. Solomon, and T. J. Kane (2009), Seasonal variation of thermospheric density and composition, *J. Geophys. Res.*, *114*, A01312, doi:10.1029/2008JA013643.

Qian, L., S. C. Solomon, and J. Laštovička (2011), Progress in observations and simulations of global change in the upper atmosphere, *J. Geophys. Res.*, *116*, A00H03, doi:10.1029/2010JA016317.

Qian, L., A. G. Burns, S. C. Solomon, and W. Wang (2013), Annual/semiannual variation of the ionosphere, *Geophys. Res. Lett.*, *40*, 1928–1933, doi:10.1002/grl.50448.

Richards, P. G., J. A. Fennelly, and D. G. Torr (1994), EUVAC: A solar EUV flux model for aeronomic calculations, *J. Geophys. Res.*, *99*, 8981.

Richmond, A. D., E. C. Ridley, and R. G. Roble (1992), A thermosphere/ionosphere general circulation model with coupled electrodynamics, *Geophys. Res. Lett.*, *19*, 601.

Roble, R. G., and R. E. Dickinson (1989), How will changes in carbon dioxide and methane modify the mean structure of the mesosphere and thermosphere?, *Geophys. Res. Lett.*, *16*, 1441.

Roble, R. G., and E. C. Ridley (1987), An auroral model for the NCAR thermospheric general circulation model (TGCM), *Ann. Geophys.*, *5A*(6), 369.

Roble, R. G., E. C. Ridley, A. D. Richmond, and R. E. Dickinson (1988), A coupled thermosphere/ionosphere general circulation model, *Geophys. Res. Lett.*, *15*, 1325.

Russell, C. T., J. G. Luhmann, and L. K. Jian (2010), How unprecedented a solar minimum?, *Rev. Geophys.*, *48*, RG2004, doi:10.1029/2009RG000316.

Schrijver, C. J., W. C. Livingston, T. N. Woods, and R. A. Mewaldt (2011), The minimal solar activity in 2008–2009 and its implications for long-term climate modeling, *Geophys. Res. Lett.*, *38*, L06701, doi:10.1029/2011GL046658.

Solomon, S. C., and L. Qian (2005), Solar extreme-ultraviolet irradiance for general circulation models, *J. Geophys. Res.*, *110*, A10306, doi:10.1029/2005JA011160.

Solomon, S. C., S. M. Bailey, and T. N. Woods (2001), Effect of solar soft X-rays on the lower ionosphere, *Geophys. Res. Lett.*, *28*, 2149.

Solomon, S. C., T. N. Woods, L. V. Didkovsky, J. T. Emmert, and L. Qian (2010), Anomalously low solar extreme-ultraviolet irradiance and thermospheric density during solar minimum, *Geophys. Res. Lett.*, *37*, L16103, doi:10.1029/2010GL044468.

Solomon, S. C., L. Qian, L. V. Didkovsky, R. A. Viereck, and T. N. Woods (2011), Causes of low thermospheric density during the 2007–2009 solar minimum, *J. Geophys. Res.*, *116*, A00H07, doi:10.1029/2011JA016508.

Solomon, S. C., A. G. Burns, B. A. Emery, M. G. Mlynczak, L. Qian, W. Wang, D. R. Weimer, and M. Wiltberger (2012), Modeling studies of the impact of high-speed streams and co-rotating interaction regions on the thermosphere-ionosphere, *J. Geophys. Res.*, *117*, A00L11, doi:10.1029/2011JA017417.

Tapping, K. F., and B. DeTracy (1990), The origin of the 10.7 cm flux, *Sol. Phys.*, *127*, 321.

Viereck, R. A., L. E. Floyd, P. C. Crane, T. N. Woods, B. G. Knapp, G. Rottman, M. Weber, L. C. Puga, and M. T. DeLand (2004), A composite Mg II index spanning from 1978 to 2003, *Space Weather*, *2*, S10005, doi:10.1029/2004SW000084.

Viereck, R. A., M. Snow, M. T. DeLand, M. Weber, L. Puga, and D. Bouwer (2010), Trends in solar UV and EUV irradiance: An update to the MgII Index and a comparison of proxies and data to evaluate trends of the last 11-year solar cycle, Abstract GC21B-0877 presented at 2010 Fall Meeting, AGU, San Francisco, Calif, 13–17 Dec.

Weimer, D. R. (2005a), Improved ionospheric electrodynamic models and application to calculating Joule heating rates, *J. Geophys. Res.*, *110*, A05306, doi:10.1029/2004JA010884.

Weimer, D. R. (2005b), Predicting surface geomagnetic variations using ionospheric electrodynamic models, *J. Geophys. Res.*, *110*, A12307, doi:10.1029/2005JA011270.

Weimer, D. R., B. R. Bowman, E. K. Sutton, and W. K. Tobiska (2011), Predicting global average thermospheric temperature changes resulting from auroral heating, *J. Geophys. Res.*, *116*, A01312, doi:10.1029/2010JA015685.

Woods, T. N. (2010), Irradiance variations during this solar cycle minimum, in *ASP Conference Series, SOHO-23: Understanding a Peculiar Solar Minimum*, edited by S. R. Cranmer, J. T. Hoeksema, and J. Kohl, vol. 428, 68 pp.

Woods, T. N., and G. J. Rottman (2002), Solar ultraviolet variability overtime periods of aeronomic interest, in *Atmospheres in the Solar System: Comparative Aeronomy*, *Geophys. Monogr. Ser.*, vol. 130, edited by M. Mendillo, A. Nagy, and J. H. Waite Jr., 221 pp., AGU, Washington D. C.

Woods, T. N., and G. Rottman (2005), The XUV photometer system (XPS): Solar variations during the SORCE mission, *Solar Phys.*, *230*, 345.

Woods, T. N., W. K. Tobiska, G. J. Rottman, and J. R. Worden (2000), Improved solar Lyman-α irradiance modeling from 1947 through 1999 based on UARS observations, *J. Geophys. Res.*, *105*, 27215.

Woods, T. N., F. G. Eparvier, S. M. Bailey, P. C. Chamberlin, J. Lean, G. J. Rottman, S. C. Solomon, W. K. Tobiska, and D. L. Woodraska (2005), Solar EUV Experiment (SEE): Mission overview and first results, *J. Geophys. Res.*, *110*, A01312, doi:10.1029/2004JA010765.

Woods, T. N., et al. (2011), Extreme Ultraviolet Variability Experiment (EVE) on the Solar Dynamics Observatory (SDO): Overview of science objectives, instrument design, data products, and model developments, *Solar Phys.*, *275*, 115, doi:10.1007/s11207-009-9487-6.

Yue, X., W. S. Schreiner, C. Rocken, and Y.-H. Kuo (2013), Validate the IRI2007 model by the COSMIC slant TEC data during the extremely solar minimum of 2008, *Adv. Space Res.*, *51*, 647.

Zhang, Y., and L. J. Paxton (2008), An empirical Kp-dependent global auroral model based on TIMED/GUVI FUV data, *J. Atmos. Sol. Terr. Phys.*, *70*, 1231.